Influence of Lyman-series fine-structure opacity on the K-shell spectrum and level populations of low-to-medium-Z plasmas

J. P. Apruzese, J. Davis, D. Duston, and R. W. Clark
Plasma Radiation Branch, Plasma Physics Division, Naval Research Laboratory, Code 4720, Washington, D.C. 20375
(Received 13 July 1983)

As laboratory plasmas of increasing atomic number, temperature, size, and/or density are produced, it becomes likely that the details of the doublet opacity profiles of the Lyman series will influence the K-shell level populations and spectrum. Accordingly, we have analyzed these effects for a range of plasma parameters, confined to densities low enough for Stark broadening to be unimportant. An analytic model is developed which predicts line power enhancements and level-population changes for K-shell plasmas. This model is based upon photon escape probability and collisional quenching concepts and is valid for plasmas of atomic number ~ 13—26. Additionally, an extensive set of numerical calculations of line ratios, line profiles, and level populations has been carried out for K-shell argon plasmas. Each computation was performed both with detailed fine-structure opacity profiles and with a single-Voigt-profile approximation. The results of these calculations may be scaled for plasmas of atomic number other than 18 using a simple set of rules discussed in the text.

I. INTRODUCTION

Recent years have witnessed dramatic technological advances in laboratory production of optically thick K-shell plasmas of low-to-medium-Z elements. Consistent with these developments, considerable theoretical effort has been devoted to elucidating the effects of opacity on the spectra and intrinsic properties of such plasmas. Typically—although not exclusively—the hydrogenlike and heliumlike resonance lines of the plasma are quite optically thick but the continua are optically thin in the x-ray region. Thus it is the line opacity which has properly attracted the most concern. As is well known from astrophysical literature, the precise form of the line-opacity profile—which determines the line-photon escape probability—plays a critical role in the formation of the spectrum and determination of the level populations. It is also true that—for quite specific physical reasons—regimes exit where simplified profiles such as pure Doppler may be employed with acceptable accuracy. For instance, Fig. 5(a) of Avrett and Hummer[1] reveals little difference in the steady-state source functions obtained for Voigt and Doppler profiles up to line-center optical depths of ~ 50 with a Voigt broadening parameter of 10^{-2}. One laboratory plasma counterpart of this situation would be a 1.5-mm aluminum plasma of ion density $\sim 10^{19}$ cm^{-3} and 600-eV temperature. Detailed calculations[2] have shown that here, too, a Doppler profile is adequate as a representation for line opacity. We will consider Z scaling of all specifically quoted plasma conditions below. At higher densities and/or optical depths a Voigt profile is required to adequately describe photon transport in the line wings. At still higher densities, Stark effects must be considered.[3–7] In this paper we will delineate the plasma conditions where the doublet-opacity profile due to fine structure in the Lyman lines must similarly be taken into account. We analyze the underlying physics with both analytic and numerical models, and obtain Z-scaled expressions governing the safe use of simpler opacity approximations. In Sec. II an analytic model is developed which serves two basic functions. First, it provides a physical basis for comprehending the trends which appear in the numerical results. Second, approximate but useful Z-scaled formulas expressing some of the results are obtained. In Sec. III specific numerical results for an argon plasma ($Z=18$) are presented along with a prescription for scaling them to plasmas of different atomic numbers.

II. ANALYTIC MODEL

A. Assumptions and restrictions

Both the analytic and numerical results contained in this paper are restricted to plasma regions where Stark broadening has only a small effect on photon transport and can be neglected. The calculations encompass at most a few hundred optical depths in Ly α; hence, for only the first three lines of the Lyman series will photon transport in the far line wings be significant. Stark profiles follow approximately an inverse 2.0—2.5 power law[3] as a function of frequency separation from line center; for Voigt profiles, the asymptotic limit is an inverse power of 2.0. Therefore, if the Stark width is smaller than the Doppler width, the Stark wings will generally be considerably smaller than the Lorentz wings. This criterion is presently adopted in determining the maximum density to which our calculations can be reasonably extended. We obtain a specific density for argon from the tabulated Stark profiles of Kepple and Whitney,[5] and scale the criterion analytically for different atomic numbers.

In examining the Stark profiles for Ly α, Ly β, and Ly γ, it is clear that the upper density limit is set by the

broad, double-peaked profile of Ly β. For argon, an electron density of $\sim 2\times 10^{22}$ cm^{-3} is required for the Stark width to equal the Doppler width at temperatures of maximum Ar XVIII abundance. Accordingly, the analytic theory presented below is valid only up to this density for argon and the numerical calculations described in the next section have not been carried to higher densities.

This criterion for the negligibility of Stark effects is readily Z-scalable. Griem, Blaha, and Kepple[3] found that the Stark widths expressed in Å for analogous lines from different elements scale approximately as $Z^{-5}N_e^{2/3}$ near maximum ionic abundance temperature. The Doppler width, also expressed in Å, scales as $Z^{-1.5}$ at maximum abundance temperature. Therefore, the Stark width for the first three Lyman lines will be less than the Doppler width if

$$\left[\frac{18}{Z}\right]^5\left[\frac{N_e}{2\times 10^{22}}\right]^{2/3}\leq\left[\frac{18}{Z}\right]^{1.5} \tag{1}$$

or

$$N_e\leq 5.1\times 10^{15}\,Z^{5.25}\,. \tag{2}$$

Consequently, the present results are not valid at electron densities higher than those indicated by Eq. (2).

The relative populations of the $2p_{3/2}$ and $2p_{1/2}$ fine-structure levels, which are likely to prevail under different plasma conditions, have been a subject of investigation and debate for quite a few years.[8–14] Irons[13] has summarized the status of this work. Briefly, at the high- and low-density limits, ϵ, the ratio of the $2p_{1/2}$ to $2p_{3/2}$ sublevel populations, will equal 0.5, the statistical weight ratio of the states. Rapid collisional mixing ensures statistical equilibrium at high densities, and in the low-density coronal limit there is little pumping of the $2p$ states from $2s$; therefore, statistical populations prevail because only this process can cause departures from $\epsilon=0.5$. In the intermediate density regime, ϵ may reach values as high as 0.7—0.8, although the relative effects of electron-ion and ion-ion collisions are not yet precisely determined[10] and render this conclusion still somewhat uncertain. As pointed out by Sampson[12] and Irons,[13,14] substantial optical depth will reduce any tendency for a departure from statistical equilibrium. In view of the remaining uncertainties as well as the fact that the plasmas we analyze here are generally optically thick, we have assumed statistical population of the $j=\frac{1}{2}$ and $j=\frac{3}{2}$ sublevels ($\epsilon=0.5$) for all the plasmas considered here, for each hydrogenlike level. We also assume that the ion thermal velocities are sufficiently greater than the plasma differential motion to enable the plasma to be treated as stationary. Irons[13,14] has explored some of the consequences of substantial plasma differential motion for Ly-α opacity.

B. Analysis of opacity effects

The doublet splitting of the Lyman series is important as an opacity determinant when the separation of the components is comparable to the Doppler half-width ($\Delta\nu_D$) of the line. For specificity, the $\Delta\nu_D$ referred to here is the half-width of the Doppler line profile at e^{-1} of the central maximum. As pointed out by Irons,[13] the ratio of the fine-structure splitting to the Doppler half-width varies as $Z^{1.5}$ since the characteristic temperature for hydrogenlike-ion predominance varies as Z^2. Specifically, for Ly α,

$$(\Delta\nu)_f/(\Delta\nu)_D\approx 5.3\left[\frac{Z}{18}\right]^{1.5}. \tag{3}$$

For Ly β, the splitting relative to the Doppler width is about one-fourth the above value; for Ly γ, about one-tenth. Therefore, fine-structure opacity effects will have by far their greatest impact on Ly α, both because of its greater optical depth and because the splitting is greater relative to the Doppler line width. Our semiquantitative analytic model consequently focuses on Ly α.

Consider the $n=2$ hydrogenlike level, with the sublevels assumed statistically populated. For the moderate density plasmas considered here, this level is populated primarily by collisional excitation from the hydrogenlike ground state and by radiative excitation due to scattered Ly α photons. Depopulation occurs by a variety of processes, including spontaneous decay, collisional excitation and de-excitation, and (primarily collisional) ionization. We will follow the standard approximate procedure in accounting for radiative excitation by diluting the spontaneous decay rate A_{21} by the spatially averaged photon-escape probability P_e. This counts only those decays not resulting in re-excitation of the $n=2$ level. Letting C_{12} stand for the collisional excitation rate from $n=1$ in cm^3 sec^{-1}, D_2 represents the sum of all collisional processes depopulating the $n=2$ level; also in cm^3 sec^{-1}, a qualitatively correct equation for the steady-state population of the $n=2$ level is

$$N_1C_{12}N_e=N_2(A_{21}P_e+D_2N_e)\,. \tag{4}$$

In Eq. (4), N_1 and N_2 are the $n=1$ and 2 level population densities (cm^{-3}), N_e is the electron density (cm^{-3}), and the other symbols are defined above. It is useful to define a quenching probability P_Q—the probability that the $n=2$ level is collisionally depopulated during a Ly-α scattering

$$P_Q=D_2N_e/(A_{21}+D_2N_e)\,. \tag{5}$$

Combining Eqs. (4) and (5) leads to the following expression for the $n=2$ population density:

$$N_2=\frac{N_1C_{12}}{D_2}\left[1\Big/P_e\left[\frac{1-P_Q}{P_Q}\right]+1\right]. \tag{6}$$

The significance of Eq. (6) becomes apparent when considering P_e. The escape probability obtained will depend on whether the single-Voigt-profile approximation or the true fine-structure profile is used in the calculation. Letting P_e now stand for the escape probability, which would be obtained from the spurious single-Voigt-profile approximation, and P_{ef} refer to the true fine-structure-opacity escape probability, the ratio of population densities obtained with the correct opacity to that obtained with the single-profile opacity is

$$\frac{N_2(\text{with fine structure})}{N_2(\text{single Voigt})}=\frac{P_e(1-P_Q)+P_Q}{P_{ef}(1-P_Q)+P_Q}\,. \tag{7}$$

Equation (7) is obtainable from Eq. (6) with the (excellent) assumption that N_1 is not affected by fine-structure opacity. Note the limits implicit in Eq. (7). At very high densities, when $P_Q \to 1$, there is no difference in populations. Collisional processes control the level population. Also, when $P_e(1-P_Q)$ and $P_{ef}(1-P_Q)$ are both much smaller than P_Q, fine structure again has no effect on N_2. This corresponds to the effectively thick case, where most photons do not escape, even after many scatterings. The number of radiative excitations, while possibly large, is determined by collisional quenching, not by the detailed behavior of P_e or P_{ef}. However, when $P_Q \to 0$ the computed populations of $n=2$ are inversely proportional to the ratio of escape probabilities. Radiative excitation dominates the level if P_e (or P_{ef}) is substantially smaller than unity. For fine-structure opacity to be negligible (defined as having less than a 10% effect on population of $n=2$) we require

$$P_e(1-P_Q)+P_Q > 0.9P_{ef}(1-P_Q)+0.9P_Q \ . \tag{8}$$

In general, P_{ef} will exceed P_e. For Ly α, a single line of optical depth τ_0 is in effect replaced by two separate lines of optical depths $\frac{2}{3}\tau_0$ and $\frac{1}{3}\tau_0$ for $2p_{3/2}$ and $2p_{1/2}$, respectively. The escape probability at large optical depth for a Voigt profile is proportional to $\tau^{-1/2}$; hence, if there is no overlap of the doublet wings

$$\frac{P_{ef}}{P_e} = \left[\frac{1}{3}\left[\frac{\tau_0}{3}\right]^{-1/2} + \frac{2}{3}\left[\frac{2\tau_0}{3}\right]^{-1/2} \Big/ (\tau_0)^{-1/2}\right] \approx 1.4 \ . \tag{9}$$

As discussed by Irons,[14] the assumption of no wing overlap fails for $\tau_0 \geq 10^2$; this failure will arise at lower τ_0 for small Z and higher τ_0 for large Z, according to Eq. (3) for the doublet spacing. However, since we seek a criterion for the *onset* of fine-structure-opacity effects, the ratio of Eq. (9) will be presently assumed. More exact results are given below in the section on numerical modeling. Combining Eqs. (8) and (9) yields the following criterion for the negligibility of fine-structure-opacity effects on population densities:

$$0.38\left[\frac{P_Q}{1-P_Q}\right] > P_e \ , \tag{10}$$

or employing Eq. (5)

$$0.38\left[\frac{D_2 N_e}{A_{21}}\right] > P_e \ . \tag{11}$$

To cast Eq. (11) into a more useful form, note that $A_{21} \approx 5\times 10^{13}(Z/18)^4$ sec^{-1}. Also, depopulation of the $n=2$ level is temperature, density, and Z dependent. Following Refs. 9–11, we will refer to the temperature in units of Z^2 Ry$=13.6Z^2$ eV. For temperatures of $(0.18$–$0.57)Z^2$ Ry (0.8 to 2.5 keV for argon) the depopulation of $n=2$, summed over the levels, has been calculated from the Coulomb-Born approximation[16] and is found to vary less than 20% from its value at $0.3Z^2$ Ry, where

$$D_2 = 2\times 10^{-10}\left[\frac{18}{Z}\right]^3 \tag{12}$$

in units of cm^{3}sec^{-1}. The temperature range $(0.18$–$0.57)Z^2$ Ry covers a large range of plasmas where hydrogenlike species are significantly present. Combining Eqs. (11) and (12) yields our final, Z-dependent criterion for less than 10% level population change due to fine-structure opacity

$$9.3\times 10^{-16} Z^{-7} N_e > P_e \ . \tag{13}$$

If the electron density is sufficiently high to render the inequality of Eq. (13) valid, fine-structure opacity—as compared to the single-Voigt-profile approximation—will affect the level populations by less than 10%. We again stress that Eq. (13) is to be applied to optically thick plasmas only—when the plasma is optically thin the fine-structure profiles cannot affect populations. The Voigt-profile escape probability P_e has been given in approximate analytic form by Athay.[15]

The effect on line emission of the doublet profile is perhaps of even more interest and importance than the change in population densities. Even though the populations may not be affected, the different effective escape probability can surely influence the Ly-α integrated intensity. The ratio of computed emission with fine-structure opacity to that obtained from a single Voigt profile is

$$\frac{I_f}{I_0} = \frac{N_2(\text{fine})A_{21}P_{ef}}{N_2(\text{single Voigt})A_{21}P_e} \ , \tag{14}$$

or, using Eq. (7),

$$\frac{I_f}{I_0} = \frac{P_{ef}}{P_e}\left[P_e + \frac{P_Q}{1-P_Q}\right] \Big/ \left[P_{ef} + \frac{P_Q}{1-P_Q}\right] . \tag{15}$$

The quantity $P_Q/(1-P_Q)$ is obtainable as above for the temperature range $(0.18$–$0.57)Z^2$ Ry, from Eqs. (5) and (12), and the expression for A_{21}

$$\left[\frac{P_Q}{1-P_Q}\right] \approx 2.45\times 10^{-15} N_e Z^{-7} \ . \tag{16}$$

Therefore,

$$\frac{I_f}{I_0} = \frac{P_{ef}}{P_e}\frac{P_e + 2.45\times 10^{-15} N_e Z^{-7}}{P_{ef} + 2.45\times 10^{-15} N_e Z^{-7}} \ . \tag{17}$$

Equation (17) is usable if P_e and P_{ef} can be calculated or estimated. If, as before, we assume $P_{ef} = 1.4P_e$ an approximate criterion for 10% enhancement of emission due to fine structure is obtainable,

$$5.2\times 10^{-15} N_e Z^{-7} > P_e \ . \tag{18}$$

The physical content of Eq. (18) is that, in an optically thick plasma with an electron density sufficiently high to validate the inequality, fine-structure opacity will result in a Ly-α intensity at least 10% higher than would be obtained from the single Voigt approximation.

We have demonstrated that the interplay of optical depth (as expressed by P_e) and the collisional quenching rate (as expressed by N_e), rather than either factor alone,

determines the importance of doublet-opacity effects on population densities and spectral emission. Several simple expressions obtained above express this interplay semiquantitatively and convincingly demonstrate the trends to be anticipated. We now turn to specific numerical results for further illumination of the question.

III. NUMERICAL MODEL

A. Model description

In order to validate and clarify the analytic approximations presented above, as well as provide more specific spectral diagnostics, we have performed an extensive series of numerical calculations centered on one element (argon). The calculations consist of a set of simultaneous solutions of the coupled atomic-rate and radiative-transfer equations for argon plasma cylinders where the varied parameters are temperature, density, and radius r, presumed much smaller than the length. These solutions have typically been carried out with both the more realistic doublet opacity and an assumed single Voigt profile for each parameter set.

The atomic model consists of 38 levels ranging from neutral Ar I to the bare nucleus (Ar XIX). Since our focus is on K-shell radiation, only ground states are carried through Be-like argon (Ar XV). For Li-like Ar XVI, the $1s^2 2s$, $1s^2 2p$, $1s^2 3s$, $1s^2 3p$, $1s^2 3d$, and $1s^2$, $n=4$ (composite) levels are modeled. The Ar XVII manifold includes $1s^2\,{}^1S$, $1s2s\,{}^3S$, $1s2p\,{}^3P$, $1s2s\,{}^1S$, $1s2p\,{}^1P$, the $n=3$ triplets and singlets, and $n=4$–7 composite levels. For Ar XVIII, $n=1$–5 are included. The various levels are connected through electron collisional excitation and deexcitation, collisional ionization and radiative recombination, three-body recombination, and, where appropriate, dielectronic recombination. Photoionization and photoexcitation are accounted for by solving the radiative transfer. All the modeled ionization edges are included as part of the radiative-transfer model. Additionally, all the optically thick resonance lines inherent in the level structure described above are also transported, along with the 2-3 line of Ar XVIII and the $1s2p\,{}^1P$–$1s3d\,{}^1D$ line of Ar XVII. While some of the higher levels have been omitted because of storage and efficiency considerations, the model provides a substantially complete description of the processes which form the dominant spectral lines of K-shell argon. A discussion of the atomic rate calculations is contained in Ref. 17. In all results presented below, the plasma is assumed to be in collisional-radiative equilibrium (CRE); namely, that each level-population density is in a steady state consistent with the atomic rates and photon fluxes produced by the other level populations.

Some improvements have been effected in our technique for carrying out the simultaneous, steady-state solution of the radiative-transfer and rate equations.[2,4,17–22] Reference 21 describes a multicell-coupling technique for radiative transfer in spherical and cylindrical geometries, based on frequency-integrated line escape probabilities. This method produces nearly exact solutions while employing only one ray angle and the computational equivalent of just one frequency per line. To account for doublet opacity, where escape probabilities have yet to be tabulated or fitted analytically, we have adopted a hybrid of the method of Ref. 21 and more conventional multifrequency approaches. The single-angle feature of Ref. 21 is retained but each line is divided into 17–43 frequency groups—depending on the line shape and optical depth. The coupling constants are defined in terms of individual frequencies (where the escape probability at each frequency is purely exponential) rather than individual lines. This also allows inclusion of continuum optical depths and line and continuum cross-pumping. Given the population densities a set of cell-to-cell photon coupling constants at each of more than 350 frequencies is thus obtainable.

The iteration technique by which self-consistency between the radiative-transfer and steady-state rate equations is obtained has also been significantly improved. The most straightforward and obvious procedure, using the radiation field from the previous iteration to calculate populations which then enables the radiation field to be recomputed until consistency is achieved, is known as Λ iteration. This technique is a very poor choice for low-density, high-optical-depth astrophysical problems[23] since the number of iterations required is approximately equal to the mean number of photon scatterings, which can be very large under such circumstances. However, the situation is not nearly so difficult for laboratory plasmas where the optical depths are smaller and the quenching probabilities larger than those which prevail in astrophysical situations, resulting in far fewer scatterings. We employ the mathematical equivalent of Rybicki's core-saturation method[24] and thereby render the Λ-iteration technique quite serviceable for laboratory plasma calculations. As noted by Rybicki,[24] the conceptual and computational simplicity of the technique is a very desirable feature, especially for complex multilevel problems.

To demonstrate our application of the core-saturation method for Λ iteration, we consider one line characterized by a profile-averaged photon escape probability from the plasma P_e and quenching probability P_Q. Let $N_u^{(i)}$ represent the upper level density obtained on the ith iteration and A the spontaneous decay probability. The photoexcitation rate for the ith iteration is therefore $N_u^{(i)}A(1-P_e)$. If C_u and D_u are the collisional creation and depopulation rates, respectively, for N_u, $N_u^{(i+1)}$ is obtained from the equation balancing gains and losses in the level

$$N_u^{(i+1)}(A+D_u)=C_u+N_u^{(i)}A(1-P_e)\,, \tag{19}$$

or

$$N_u^{(i+1)}=N_u^{(1)}+N_u^{(i)}(1-P_e)(1-P_Q)\,, \tag{20}$$

where $P_Q=D_u/(A+D_u)$ as before, and the upper level population for an optically thin plasma is given by the first iterative solution

$$N_u^{(1)}=\left[\frac{C_u}{A+D_u}\right]. \tag{21}$$

Equation (20) yields a recursive sum for the nth iteration's solution

$$N_u^{(n)}=N_u^{(1)}\sum_{i=0}^{n-1}[(1-P_e)(1-P_Q)]^i . \tag{22}$$

The slow convergence of the sum of Eq. (22) when $P_e, P_Q \ll 1$ precisely expresses the difficulty of Λ iteration. Note, however, that the sum is analytically evaluable to give

$$N_u^{(\infty)}=N_u^{(1)}\left[\frac{1}{1-(1-P_Q)(1-P_e)}\right] \tag{23}$$

and that this is exactly what is obtained for N_u on the *first* iteration if, in Eq. (19) A is replaced by AP_e instead of calculating excitations as $A(1-P_e)$. This is the essence of Rybicki's technique[24] of eliminating the readily absorbed line core photons. In practice, we apply the method by calculating, cell by cell, the escape probability from the plasma for each line by integrating over the absorption profile—including the continuum. The spontaneous emission coefficients are then diluted by this factor on the first iteration, which generally results in an excellent approximation to the final solution, especially near the plasma center. On subsequent iterations, the spontaneous emission coefficients are diluted in each cell by the escape probability from that cell and excitations are computed explicitly only for the line wing photons arriving from other cells. This completely general procedure usually converges within 20 iterations even for several hundred Ly-α optical depths. Convergence has been verified by starting with entirely different initial iterative solutions, and by quadrupling the number of iterations, both of which yield the same final level populations.

B. Z scaling of numerical results

In order that the results given below, specifically obtained for argon, may be readily applied to other low-to-medium-Z elements, we present the methodology for Z scaling in this section. Given a K-shell argon plasma of radius R_0, ion density N_I, and temperature T_e, the results may clearly be applied to a plasma of atomic number Z at a temperature of $T_e(Z/18)^2$. However, scaling the density and size is not quite so straightforward. To maintain the analogous level populations and spectrum, it is evident from the discussion in Sec. II that both the quenching probabilities and optical depths must remain the same. The quenching probability is determined by the ratio of collision rates—which scale as Z^{-3}—to spontaneous decay rates—which scale as Z^4. Since the quenching probability consequently scales as Z^{-7}, the electron density must scale as Z^7 to offset this. Therefore, the ion density must increase as Z^6 to maintain the same ratio of radiative to collisional rates as would prevail in an argon plasma. Finally, to maintain the same line optical depth τ_0, note that it is proportional to $R_0 N_I \lambda (M/T_I)^{1/2}$ where λ is the wavelength, M the ion mass, and T_I the ion temperature. Since $N_I \sim Z^6$, $\lambda \sim Z^{-2}$, $M \sim Z$, and $T_I \sim Z^2$, $\tau_0 \sim R_0 Z^{3.5}$. Therefore, the size must scale as $Z^{-3.5}$ to maintain the optical depth. In summary, a K-shell plasma of atomic number Z, radius $R_0(18/Z)^{3.5}$, ion density $N_I(Z/18)^6$, and temperature $T_e(Z/18)^2$ will produce the same spectrum as an argon plasma of radius R_0, ion density N_I, and electron temperature T_e. The "same" spectrum is defined as the same relative intensities of the lines. Absolute intensities will differ due to the differing line photon energies and total numbers of emitting ions. We recommend Z scaling only for $13 \lesssim Z \lesssim 26$ from the $Z=18$ results presented below, since the $Z^{1.5}$ scaling of fine-structure splitting [Eq. (3)] will spoil the applicability of the scaling far from $Z=18$.

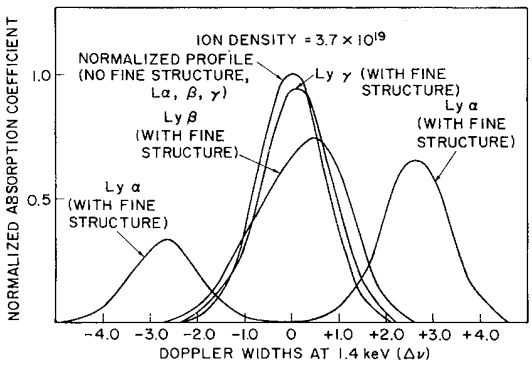

FIG. 1. Normalized fine-structure profiles of the absorption coefficients of Ar XVIII Ly α, β, and γ are compared to the single Voigt profile which would characterize the opacity in the absence of fine-structure splitting.

C. Numerical results

In Fig. 1 the doublet absorption profiles for Ar XVIII Ly α, Ly β, and Ly γ are shown along with the single Voigt profile which would characterize the line opacity in the absence of fine structure. The profiles are normalized for case of comparison. Plasma conditions of ion temperature 1.4 keV and ion density 3.7×10^{19} cm^{-3} are assumed. Note that the Ly-α profile is split into two distinct features since the doublet components are $\sim$5 Doppler widths apart. However, both Ly β and Ly γ appear quasi-Gaussian, with a skewing of the profile toward the stronger of the fine-structure components. For Ly γ, the change from the single Voigt profile is quite small.

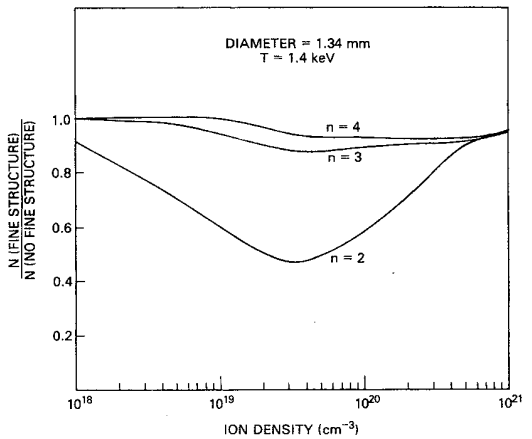

FIG. 2. Ratio of the $n=2$, 3, and 4 Ar XVIII populations obtained with the correct fine-structure profiles to those obtained using a single Voigt profile are plotted against ion density for the indicated cylindrical plasma temperature and diameter.

Therefore, the following results will concentrate on Ly-α and Ly-β power outputs and line ratios which could reflect those outputs as influenced by fine-structure opacity.

In Fig. 2 the ratio of populations calculated with realistic doublet opacities to those which would prevail in the absence of fine structure is plotted against density, for an argon plasma temperature of 1.4 keV and a diameter of 1.34 mm. The changes in $n=3$ and 4 are 15% or less, whereas, for an ion density of $\sim 3\times 10^{19}$ cm^{-3}, the $n=2$ population is reduced by a factor of 2. For all three levels, the population ratio approaches unity at both low and high densities, consistent with Eq. (7). For the $1s_{1/2}$-$2p_{3/2}$ component, the line-center optical depths are 0.14, 2, 47, and 420 at ion densities of 10^{18}, 10^{19}, 10^{20}, and 10^{21} cm^{-3}, respectively. The corresponding optical depth of a single Voigt profile, τ_0, would be 50% greater. Since $N_e \approx 18 N_I$, $\tau_0 \approx 3.5\times 10^{-20} N_e$ for ion densities between 10^{20} and 10^{21} cm^{-3}. The approximate escape probability for a Voigt profile[15] is given as a function of the damping parameter a and optical depth τ_0 for $\tau_0 \gg 1$:

$$P_e \approx 0.85 \left[\frac{a}{\tau_0} \right]^{1/2} . \tag{24}$$

The damping parameter a for a resonance line is

$$a = \frac{\Gamma}{4\pi \Delta \nu_D} , \tag{25}$$

where the upper-state inverse lifetime Γ for Ly α is mostly determined by radiative decay in this density range. The Doppler width $\Delta\nu_D$ at 1.4 keV is 2.2×10^{14} Hz. Including the collisional contribution, $a \approx 2.5\times 10^{-2}$ for these densities, and Eqs. (24) and (13) may be combined to obtain the electron density at which a 10% departure of $n=2$ population due to fine-structure opacity would be expected according to the analytic theory

$$9.3\times 10^{-16}(18)^{-7} N_e > 0.85 \left[\frac{2.5\times 10^{-2}}{3.5\times 10^{-20} N_e} \right]^{1/2} \tag{26}$$

which yields an electron density of 6.1×10^{21} cm^{-3}, equivalent to an ion density of 3.4×10^{20} cm^{-3} which is in excellent agreement, considering the approximations, with the numerically calculated value of 4.5×10^{20} (Fig. 2).

The most experimentally detectable consequence of fine structure is certainly spectroscopic effects. The analytic results presented above also contain [Eq. (18)] an electron-density criterion for 10% enhancement of Ly α. In Fig. 3 we present two line ratios which are both temperature and density sensitive: He $1s^2$—$1s4p\ ^1P$/Ly β and He $1s^2$—$1s3p\ ^1P$/Ly α, as a function of density, with and without the correct doublet opacity. The ratios decrease substantially with density even with fixed temperature (1.4 keV) and plasma diameter (1.34 mm) since higher collision rates and optical depths increase the excitation and ionization state of the plasma. However, at the highest densities the Ar XVII to Ar XVIII line ratios level off and then increase. This is primarily due to the increased opacity of the Lyman lines coupled with the decreased opacity of the heliumlike lines as the average charge state of the plasma increases with density. The double valuing of line ratios

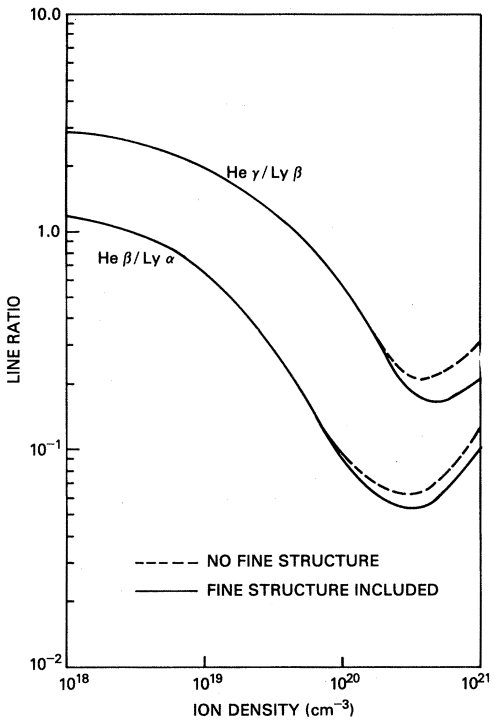

FIG. 3. Line ratios Ar XVII $1s^2$—$1s3p\ ^1P$/Ly α and Ar XVII $1s^2$—$1s4p\ ^1P$/Ly β are plotted against ion density for a plasma diameter of 1.34 mm and temperature 1.4 keV. Where fine-structure opacity results in significant differences, it is indicated.

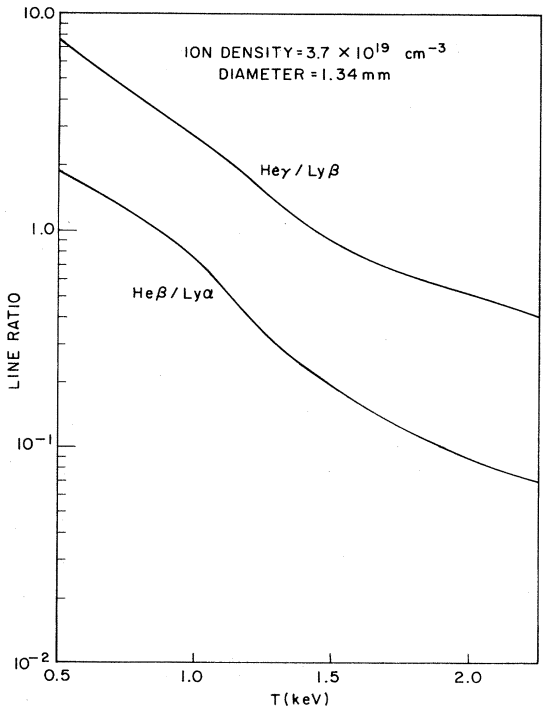

FIG. 4. Same line ratios of Fig. 3 are plotted against temperature for the same size cylindrical argon plasma (1.34 mm) at an ion density of 3.7×10^{19} cm^{-3}, where the presence of fine structure makes no difference.

due to opacity effects has been noted elsewhere.[19] At ion densities of $\sim 10^{20}$ and higher, the dichotomy between fine-structure and single-profile calculations is noticeable; it reflects the higher power outputs of both Ly α and Ly β due to the greater effective escape probabilities of the doublet profiles. For Ly α, these results provide another point of comparison with the theory of Sec. II. According to Eq. (18), the Ly-α line intensity should be enhanced by 10% when

$$5.2\times 10^{-15} N_e Z^{-7} > P_e \ . \tag{18}$$

Equation (24), plus the fact that $\tau_0 \approx 3.5\times 10^{-20} N_e$ allows Eq. (18) to be solved for N_e; the result predicts a 10% power enhancement at $N_I \approx N_e/18 = 1.1\times 10^{20}$ cm^{-3}, in excellent agreement with the numerically calculated value of 1.3×10^{20} cm^{-3} (Fig. 3).

Figures 4 and 5 present this same ratio as a function of temperature, again for a plasma of fixed diameter 1.34 mm. In Fig. 4 the ion density is 3.7×10^{19} cm^{-3}. At these relatively modest optical depths (~ 10 for Ly α) the ratios are single valued and a very good temperature indicator. Also, fine structure does not affect the power output at this density; therefore, only one curve appears for each line ratio. This may be contrasted with Fig. 5 where the same information is presented at the considerably higher ion density of 10^{21} cm^{-3}. Fine-structure opacity noticeably depresses the line ratios for the entire temperature range considered. Also, the much larger optical depths virtually eliminate the temperature sensitivity of the ratios above 1.0 keV; as the population of Ar XVIII increases with temperature, so does the opacity, which considerably reduces the tendency of the Lyman line to increase in intensity. At an ion density of 3.7×10^{19} cm^{-3}, the Lyman photons generally escape after a few scatterings; at 10^{21} cm^{-3}, they are mostly collisionally quenched.

The fact that the enhancement of Ly β is comparable to that of Ly α may seem puzzling in light of the fact that the Ly-β profile is not so drastically affected by fine structure (Fig. 1). However, the Lorentz wings of the profile are substantially enhanced by the increase in damping parameter (i.e., reduction in level lifetime) when collisions transferring population among fine-structure levels are considered. At such high opacities, substantial numbers of photons can escape only in these far wings—resulting in the Ly-β power increase. For Ly α, as noted above, the upper level lifetime is still mostly determined by its very high radiative decay rate, even when collisions among fine-structure levels are considered.

Finally, in Fig. 6 we present the evolution of the emitted Ly-α profile as a function of density for a temperature of 1.4 keV and a plasma diameter of 1.34 mm. At $N_I = 10^{18}$ cm^{-3}, the $2p_{3/2}$ component is twice the strength of the $2p_{1/2}$ since the lines are optically thin at this density. At 6×10^{18} cm^{-3}, $\tau_0 \approx 1$ and the $2p_{3/2}$ component begins to saturate to the value of the source function—allowing the $2p_{1/2}$ to begin to approach its intensity. At 3.7×10^{19} cm^{-3}, full saturation has occurred—the components are of equal intensity and a small self-reversed core is seen in each. The profiles at ion densities of 10^{20} and 3×10^{20} cm^{-3} are qualitatively similar to that at

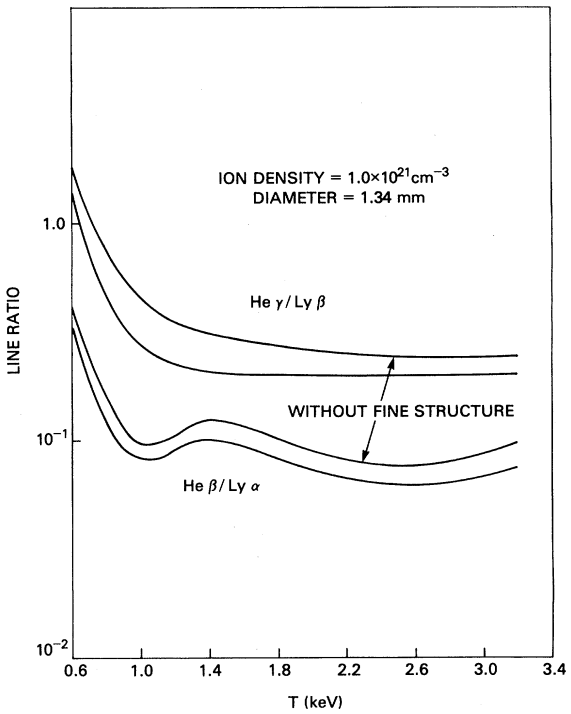

FIG. 5. Same as Fig. 4, except the density is 10^{21} ions per cm^{-3}. At this density the result depends upon the details of the fine-structure profile and such is indicated.

3.7×10^{19} cm^{-3} except that the higher optical depths produce deeper self-reversed cores. At ion densities of 7.5×10^{20} cm^{-3} and 10^{21} cm^{-3}, the profiles have a peculiar three-pronged appearance. The three peaks appear where the profile optical depth is approximately unity—one peak on each of the far wings of the components, with another emission peak occurring at the absorption minimum between the two components.

Because of this density sensitivity, the Ly-α profile is potentially an excellent density diagnostic. Since the pro-

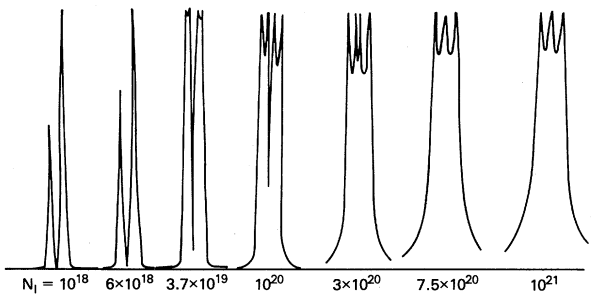

FIG. 6. Evolution of the emitted Ly-α profile is presented as a function of density for an argon plasma of 1.4 KeV and diameter 1.34 mm. The splitting of the two components (visible at the lowest density) is 5.4 mÅ and this horizontal scale is maintained throughout. The absolute intensities have been normalized for ease of comparison.

files depend on optical depth as well as density, the size of the plasma must be ascertained to fully exploit this technique. Experimental methods such as x-ray pinhole photography would be quite valuable for this purpose. Also, spectral resolution of $\sim 1-2$ mÅ will be required, independently of Z.

ACKNOWLEDGMENTS

The authors would like to express their appreciation to Dr. P. C. Kepple and Dr. H. R. Griem for several valuable discussions. This work was supported by the U. S. Defense Nuclear Agency.

[1]E. H. Avrett and D. G. Hummer, Mon. Not. R. Astron. Soc. 130, 295 (1965).
[2]J. P. Apruzese, J. Davis, D. Duston, and K. G. Whitney, J. Quant. Spectrosc. Radiat. Transfer 23, 479 (1980).
[3]H. R. Griem, M. Blaha, and P. C. Kepple, Phys. Rev. A 19, 2421 (1979).
[4]J. P. Apruzese, P. C. Kepple, K. G. Whitney, J. Davis, and D. Duston, Phys. Rev. A 24, 1001 (1981).
[5]P. C. Kepple and K. G. Whitney, Naval Research Laboratory (NRL) Memorandum Report No. 4565, 1981 (unpublished).
[6]A. Hauer, K. G. Whitney, P. C. Kepple, and J. Davis, Phys. Rev. A 28, 963 (1983).
[7]R. W. Lee, J. Quant. Spectrosc. Radiat. Transfer 27, 87 (1982).
[8]R. J. Hutcheon and R. W. P. McWhirter, J. Phys. B 6, 2668 (1973).
[9]I. L. Beigman, V. A. Boiko, S. A. Pikuz, and A. Ya. Faenov, Zh. Eksp. Teor. Fiz. 71, 975 (1976) [Sov. Phys.—JETP 44, 511 (1976)].
[10]A. V. Vinogradov, I. Yu. Skobelev, and E. A. Yukov, Fiz. Plazmy 3, 686 (1977) [Sov. J. Plasma Phys. 3, 389 (1977)].
[11]V. A. Boiko, A. V. Vinogradov, S. A. Pikuz, I. Yu. Skobelev, A. Ya. Faenov, and E. A. Yukov, Fiz. Plasmy 4, 97 (1978) [Sov. J. Plasma Phys. 4, 54 (1978)].
[12]D. H. Sampson, J. Phys. B 10, 749 (1977).
[13]F. E. Irons, Aust. J. Phys. 33, 283 (1980).
[14]F. E. Irons, J. Quant. Spectrosc. Radiat. Transfer 24, 119 (1980).
[15]R. G. Athay, *Radiation Transport in Spectral Lines* (Reidel, Dordrecht, 1974), pp. 22—24.
[16]L. A. Vainshtein and I. I. Sobel'man, Lebedev Report No. 66, 1967 (unpublished); I. I. Sobel'man, *Introduction to the Theory of Atomic Spectra* (Pergamon, New York, 1972).
[17]D. Duston and J. Davis, J. Quant. Spectrosc. Radiat. Transfer 27, 267 (1982).
[18]J. P. Apruzese, J. Davis, and K. G. Whitney, J. Appl. Phys. 48, 667 (1977).
[19]D. Duston and J. Davis, Phys. Rev. A 21, 932 (1980).
[20]K. G. Whitney, J. Davis, and J. P. Apruzese, Phys. Rev. A 22, 2196 (1980).
[21]J. P. Apruzese, J. Quant. Spectrosc. Radiat. Transfer 25, 419 (1981).
[22]D. Duston, J. Davis, and P. C. Kepple, Phys. Rev. A 24, 1505 (1981).
[23]D. Mihalas, *Stellar Atmospheres* (Freeman, San Francisco, 1970), pp. 152—155.
[24]G. B. Rybicki, Conference on Line Formation in the Presence of Magnetic Fields, National Center for Atmospheric Research Report, Boulder, 1971 (unpublished).